



1 Article

## 2 Inks development for 3D printing cathode of Li-ion 3 microbatteries

4 Maxim Maximov <sup>1,\*</sup>, Denis Kolchanov <sup>2</sup>, Ilya Mitrofanov <sup>1</sup>, Alexander Vinogradov <sup>2</sup>, Yury  
5 Koshtyal <sup>3</sup>, Alexander Rymyantsev <sup>1</sup>, Anatoly Popovich <sup>1\*</sup>

6 <sup>1</sup> Peter the Great Saint-Petersburg Polytechnic University, Saint-Petersburg (SPbPU), Russian Federation;  
7 [maximspbstu@mail.ru](mailto:maximspbstu@mail.ru) (M.M.), [carlemeros@gmail.com](mailto:carlemeros@gmail.com) (I.M.)

8 <sup>2</sup> ITMO University St. Petersburg, Russia; [kolchanov@scamt-itmo.ru](mailto:kolchanov@scamt-itmo.ru) (D.K.)

9 <sup>3</sup> National Technology Initiative Center of Excellence in Advanced Manufacturing Technologies at Peter the  
10 Great St. Petersburg Polytechnic University (Y.K.)

11 \* Correspondence: [maximspbstu@mail.ru](mailto:maximspbstu@mail.ru)

12 Academic Editor: name

13 Received: date; Accepted: date; Published: date

14 **Abstract:** Due to the demand for wearable and implantable microelectronic devices (MED), there is  
15 a growing interest in the development of thin-film lithium-ion microbatteries (LiBs) with  
16 high-energy density. The high cost of production is an issue restraining thin-film LiBs wide  
17 application. Inkjet printing is a method of applying materials to the substrate surface: ink droplets  
18 formed on piezoelectric nozzles fall on the substrate, whereafter evaporation of the solvent thin  
19 layer of film is formed. The proposed technology can simplify the production of LiBs for MED and  
20 reduce their cost. The present work reports results of inkjet printing 3D cathodes development for  
21 LiBs. The 3D printed cathodes were produced with using synthesized Li-rich cathode material  
22 ( $\text{Li}_{1.2+x}\text{Mn}_{0.54}\text{Ni}_{0.13}\text{Co}_{0.13}\text{O}_2$ ,  $0 < x < 0.05$ ) which has a larger capacity ( $>250$  mAh/g) in comparison with  
23 the materials used in modern lithium-ion cells. For LiB electrode printing the non-aqueous solvent  
24 based inks were used. The prepared cathode material was dispersed in N-methyl-2-pyrrolidone.  
25 The effect of various additives such as ethylene glycol, diethylene glycol, propylene glycol on the  
26 viscosity and stability of the ink was studied. Inkjet printing was performed with the use of  
27 Dimatix Material Printer 2831. Substrate temperature, number of layers and other parameters were  
28 varied to determine the optimal printing conditions.

29 **Keywords:** Lithium-ion microbatteries, 3D printing cathode, Li-Rich cathode, Inkjet printing LiBs  
30

---

### 31 1. Introduction

32 Currently, due to the development of wearable and implantable microelectronic devices:  
33 biomedical implants, autonomous sensors, smart cards, chips with built-in power sources etc. there  
34 is a growing interest to research and development of solid-state thin-film Li-ion batteries (LiBs). In  
35 order to be applied for powering microelectronic devices (MED) the developed LiBs should meet  
36 requirements such as reduced dimensions, high energy density, cycle life, costs of production and so  
37 on. For better satisfaction of these requirements the new technologies and approaches of LiBs  
38 production should be developed. For the mass production, the possibility of scaling and simplifying  
39 of LiBs manufacturing technology are important advantages.

40 Modern methods of 3D printing (inkjet printing) allow to deposit thin (including films with a  
41 thickness less than 1  $\mu\text{m}$ ) films with different compositions and functions such as cathodes, anodes  
42 and electrolytes. The sequential application of different functional layers can be effectuated to obtain  
43 elementary cells which can be combined into a battery [1].

44 During inkjet printing ink droplets formed on piezoelectric nozzles fall on the substrate,  
45 whereafter evaporation of the solvent they form a thin layer of bounded powder particles – film.  
46 This technology allows using a wide range of solvents and particle sizes, to vary the thickness of  
47 printed objects and to use inks with complex composition. In order to provide high quality film the  
48 ink (active cathode material particles dispersed in liquid) no sedimentation should occur during  
49 relatively long period of time.

50 Lithium and manganese rich (LMR) cathode materials  $\text{Li}_2\text{MnO}_3$  ( $\text{Li}[\text{Li}_{1/3}\text{Mn}_{2/3}]\text{O}_2$ )  $\times$   $\text{LiMO}_2$  ( $M =$   
51  $\text{Ni, Co, Mn}$ ) have an increased specific discharge capacity (250-270 mAh/g, 2.0-4.8V) [2-4]. After  
52 activation [2,5,6], (charge at 4.5-4.6 and higher at low C-rates) of  $\text{Li}_2\text{MnO}_3$  LMR can exhibit increased  
53 capacity in narrow voltage window. Low cobalt content and higher content of cheaper manganese  
54 can reduce the price of LIBs. Thanks to the marked advantages this class of materials attracts  
55 attention of developers of lithium-ion cells made by traditional technology and can be also used in  
56 development of solid-state batteries.

## 57 2. Materials and Methods

58 The cathode materials  $\text{Li}_{1.2-x}\text{Mn}_{0.54}\text{Ni}_{0.13}\text{Co}_{0.13}\text{O}_2$  ( $x=0; 0,05$ , denoted as 1.20NCM and  
59 1.25NCM) were synthesized by the sol-gel method. The stoichiometric amount of  
60  $\text{Li}(\text{CH}_3\text{COO})\cdot 2\text{H}_2\text{O}$ ,  $\text{Ni}(\text{CH}_3\text{COO})_2\cdot 4(\text{H}_2\text{O})$ ,  $\text{Co}(\text{CH}_3\text{COO})_2\cdot 4(\text{H}_2\text{O})$ ,  $\text{Mn}(\text{CH}_3\text{COO})_2\cdot 4(\text{H}_2\text{O})$  was  
61 dissolved in 0.4M citric acid solution stirred with use of magnetic stirrer. The resulting solution was  
62 dried in vacuo for 6 hours at 100°C until the complete evaporation of solvent. Then the obtained  
63 mixtures were heat treated in the air atmosphere according to the following program: heating rate 10  
64 deg/min to 400°C, holding for 4 hours at 400°C, 10 deg/min to 800°C, holding for 6 hours at 800°C.

65 The crystal structure of cathode material was analyzed by X-ray diffraction (XRD) of Cu  $K\alpha$   
66 radiation with use of Bruker D8 Discover. The scan range was 15-70 ( $2\theta$  degrees) at a scan speed of  
67 10 °/min. In order to calculate lattice parameters the Rietveld refinement was used. The crystal size  
68 was estimated from Scherrer equation. The morphology of the cathode materials was investigated  
69 by scanning electron microscopy (SEM, Zeiss SUPRA 40VP) in «Centre for X-ray Diffraction  
70 Studies» and «interdisciplinary resource centre for nanotechnology» respectively of the research  
71 park of Saint-Petersburg University. The element composition was identified by energy dispersive  
72 X-ray spectroscopy (EDS). Particle size distribution of as-synthesized and ground (loading 1:200,  
73 300rpm, 0.5 hour, Pulverisette 4) material was measured by laser scattering with use of Analysette  
74 Nanotec 22 (Fritsch).

75 To evaluate the electrochemical performance of synthesized materials the electrodes were  
76 prepared by method which is similar to the used in lithium ion cells manufacturing. The active mass  
77 was prepared by mixing 80 wt% active materials, 10 wt% carbon black, and 10 wt% polyvinylidene  
78 fluoride (PVDF) and vigorously stirred in N-methyl pyrrolidinone (NMP) to obtain a slurry. The  
79 slurry was evenly spread on an Al foil with use of Dr. Blade. The prepared electrodes were dried,  
80 calendered and cut down. Prior to assembly, the electrodes were dried at 110° C for 12 h in a vacuum  
81 oven. The electrochemical testing was made in CR-2032-coin cells assembled in an argon filled glove  
82 box. Lithium foil was used as counter electrode TC-E918 (Tinci), Cellgard 2335 were used as the  
83 electrolyte and the separator, correspondingly.

84 Electrochemical tests were performed using Neware CT-3008-5V1mA-164 test system at 0.1C  
85 current rate in potential range of 2.5-4.8 V at room temperature. Stepwise activation of the cathode  
86 material was carried out to obtain high specific capacity values.

87 To prepare ink for printing, 3.2 ml of N-methyl-2-pyrrolidone was added to 160 mg of the active  
88 cathode the obtained slurry was dispersed in an ultrasonic bath for 3 hours. Large agglomerates of  
89 particles were removed by centrifugation for 10 minutes at 5000 RPM the precipitate was removed  
90 and weighed to determine the exact concentration of a colloidal solution. The particle size  
91 distribution was measured by dynamic light scattering (Photocor Compact-Z). Carbon nanotubes  
92 (CNT) were used as a conductive additive, 20 mg CNT were dissolved in 0.4 ml  
93 N-methyl-2-pyrrolidone and dispersed in an ultrasonic bath for 15 minutes. Polyvinylidene fluoride  
94 (PVDF) was used as a binding agent, 20 mg PVDF was dissolved in 0.4 ml N-methyl-2-pyrrolidone.

95 In order to obtain ink the prepared solutions were mixed in a weight ratio of 8:1:1. The viscosity  
96 of the ink was controlled by the addition of various components to the original mixture: ethylene  
97 glycol, diethylene glycol, propylene glycol, and was measured using the Fungilab Expert  
98 viscometer, Spain.

99 The stability of the ink was evaluated by measuring the  $\zeta$ -potential on the Photocor Compact-Z  
100 device, which contains a 2 ml sample cell in which carbon electrodes are placed. The principle of  
101  $\zeta$ -potential measurement is based on the method of dynamic light scattering in the mode of velocity  
102 flow measurement.

103 Surface tension was measured by the hanging drop method on the KRUSS DSA25.

104 The cathode for LiBs was printed on an inkjet printer Dimatix Material printer 2831 using  
105 Dimatix material cartridge with a drop volume of 10 pl. The inks used for printing fulfilled the  
106 requirements to viscosity (8-10 cPs) and surface tension (28-32 mN/m).

107 Inkjet printing of the cathode was carried out on aluminum foil. The quality of inkjet printing  
108 was regulated by changing the drop spacing (DS) and the number of layers. To create a high-quality  
109 electrode coating, the optimal printing parameters were selected: DS 50  $\mu\text{m}$ , the number of layers 20.

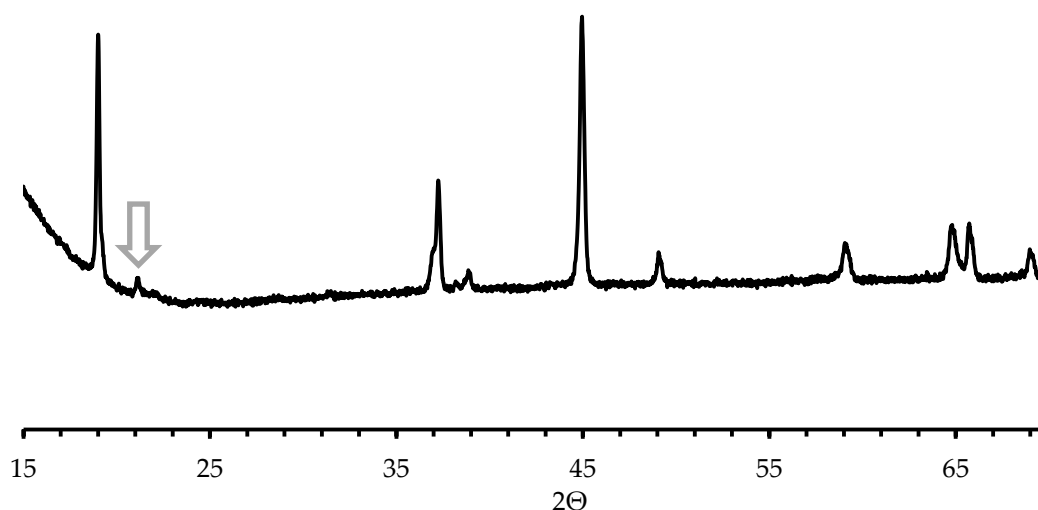
### 110 3. Results and discussion

#### 111 3.1. Characterization of the cathode material

112 The position and number of reflexes presented on the XRD pattern (Figure 1) correspond to  
113 LMR material [7]. The reflections manifested in the region of 20-23  $^\circ$  ( $2\Theta$ ) show the presence of a  
114 monoclinic phase of  $\text{Li}_2\text{MnO}_3$  with the spatial group C2/m in the sample composition. The crystal  
115 lattice parameters of the samples:  $a = 2.845 \div 2.842 \text{ \AA}$ ,  $c = 14.231 \div 14.233 \text{ \AA}$ , The volume of the  
116 crystalline cells is about  $100.1 \text{ \AA}^3$ , the crystallite size is of the order of 50 nm.

117 The phase composition corresponds to the phase composition of cathode materials enriched  
118 with lithium and manganese According to the XRD, there are two phases in the material structure -  
119  $\text{Li}_2\text{MnO}_3$  and  $\text{LiMO}_2$ . The intensity of the I003 / I104 maxima varied from 0.58 to 0.66.

120

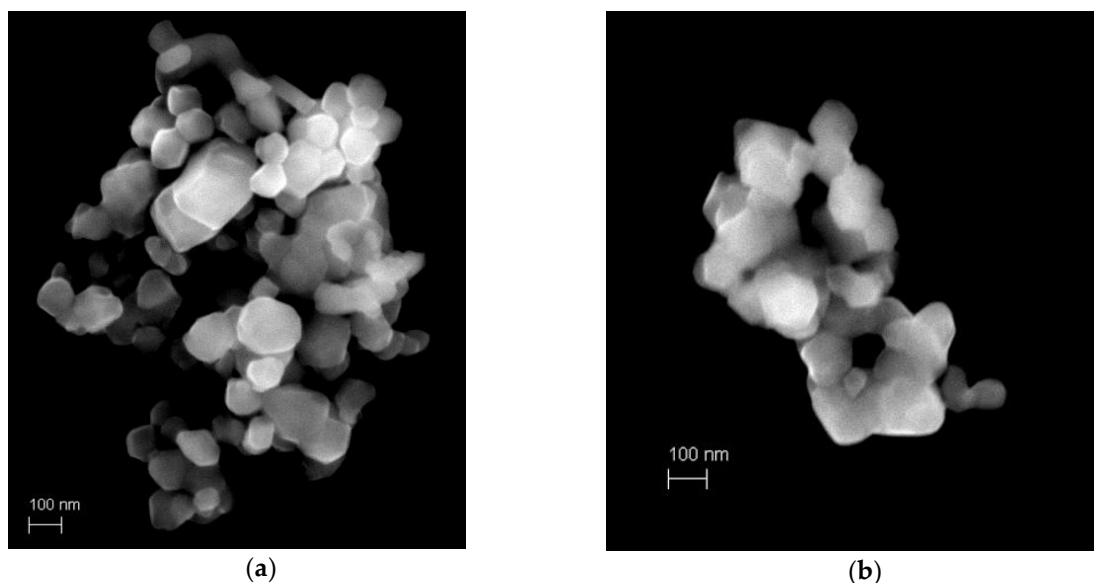


121

122 **Figure 1.** The XRD pattern of the 1.25 NCM

123 The synthesized cathode material comprised of big size agglomerates (10-100  $\mu\text{m}$ ). Before  
124 preparing the active mass, the cathode materials were ground in a planetary mill. The particle size  
125 distribution of ground materials has following parameters: D10 – 0.1  $\mu\text{m}$ , D50 – 0.2  $\mu\text{m}$ , D90 – 0.7  
126  $\mu\text{m}$ .

127 According to SEM images (Figure 2) the ground powder confirms the presence of a significant  
128 number of particles smaller than 200 nm, including particles of the order of 50 nm. In accordance  
129 with the results of energy-dispersive spectroscopy, transition metals – nickel, cobalt and manganese  
130 are present in the material in a ratio proportional to the stoichiometric coefficients in the formula.  
131



132 **Figure 2.** The SEM pattern of the 1.25 NCM(a) and 1.20 NCM(b)

### 133 3.2. Electrochemical performance

134 For carrying out electrochemical tests, coin cells with positive electrodes fabricated according to  
135 the generally know method were assembled. Before activation process both samples (1.2NCM and  
136 1.25NCM) exhibited moderate values of discharge capacity (80 mAh/g – 4.2V, 105 mAh/g) – 4.4V).  
137 After activation process the discharged capacities increased to 160 mAh/g (4.2V), 180 mAh/g (4.4V)  
138 and >250 mAh/g (4.8V). The 1.2NCM showed slightly higher discharge capacity. Coulomb efficiency  
139 of primary cycles after activation was 98.5-99.5%.

### 140 3.3. Formulation of ink for inkjet printing

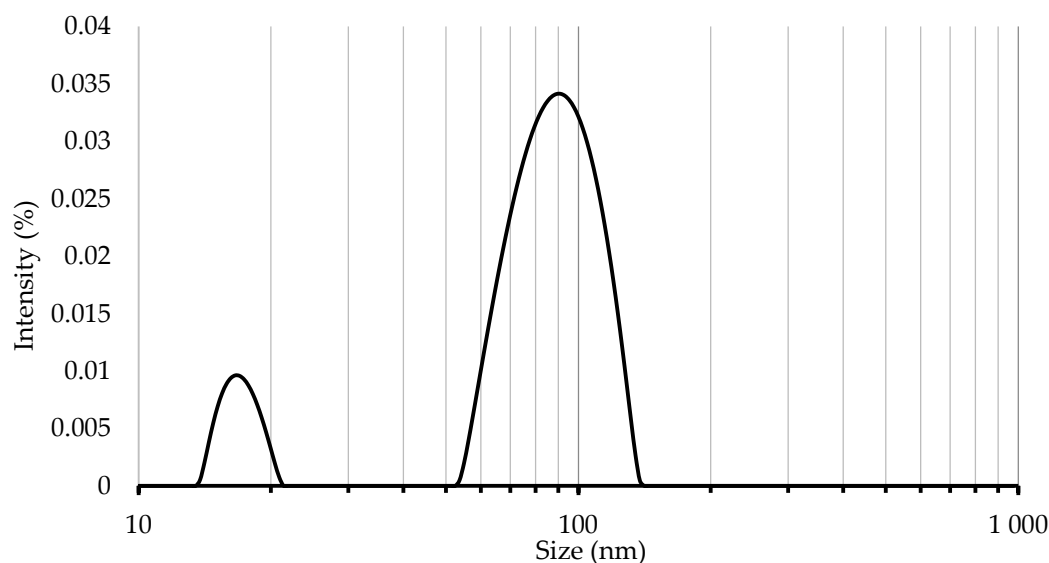
141 In the course of the investigation, the colloid solution of cathode material was adapted for inkjet  
142 printing. A particle size distribution (hydrodynamic radius) was determined. The optimal  
143 rheological parameters and ink composition for inkjet printing were found, the stability of the  
144 selected composition was investigated.

#### 145 3.3.1. Particle size control

146 After separation of large agglomerates of ground cathode material (1.2NCM) by centrifugation  
147 the solution contained agglomerates with size less than 140 nm (Figure 3). The particle size  
148 distribution and the maximum particle size meet the requirements for ink which must be fulfilled to  
149 conduct inkjet printing.

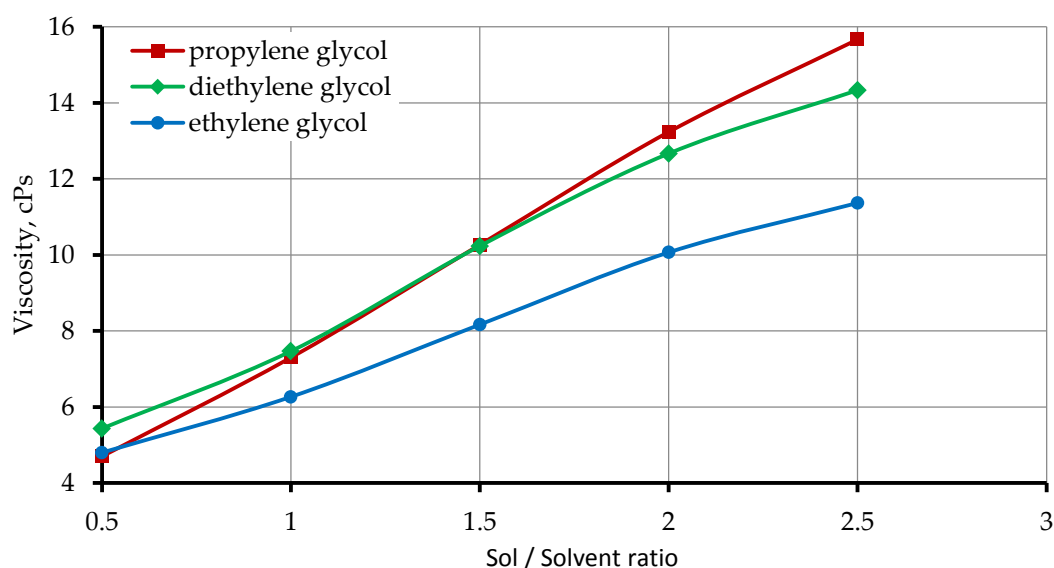
#### 150 3.3.2. Control of rheological properties

151 The effect of the addition of different solvents to the original sol on the ink viscosity was  
152 investigated (Figure 4).



153  
154  
155  
156

Figure 3. The hydrodynamic size of cathode material particles



157  
158  
159  
160  
161  
162  
163

Figure 4. The effect of sol/solvent ration on the ink viscosity

The compositions of the ink with a viscosity of 8-10 cPs satisfy the printing conditions.

Surface tension plays an important role in the formation of drops, and the stability of the ink indicates their suitability for printing. Ink stability was evaluated by  $\zeta$ -potential (Table 1).

Table 1. Surface tension and  $\zeta$ -potential for ink compositions with optimum viscosity

The composition of the ink		Surface tension mN/m	$\zeta$ -potential mV
ethylene glycol	Sol	26	-18
1.5	1		
diethylene glycol	Sol	27	-24
1	1		
propylene glycol	Sol	30	-33
1	1		

164 Among the considered mixtures the propylene glycol was chosen for electrode printing since it  
165 has viscosity close to required value, more stable in time (possess lower  $\zeta$ -potential) and has highest  
166 surface tension. The printed layer had uniform distribution of material.

#### 167 4. Conclusions

168 In the course of work, the nanoscale powders of the cathode materials  $\text{Li}_{1.20}[\text{Ni}_{0.13}\text{Co}_{0.13}\text{Mn}_{0.54}]\text{O}_2$ ,  
169  $\text{Li}_{1.25}[\text{Ni}_{0.13}\text{Co}_{0.13-x}\text{Mn}_{0.54}]\text{O}_2$  was synthesized. According to X-ray diffraction, the presences of two  
170 layered crystalline phases with spatial groups R3m and C2/m were found in prepared samples. The  
171 powders of cathode materials consist of large size agglomerates (10-100  $\mu\text{m}$ ). After grinding of the  
172 agglomerated segments in a planetary mill, the size of agglomerates diminished of 100-200 nm (d50).  
173 The electrodes obtained by applying electrode paste to the aluminum foil after activation process  
174 showed a large discharged capacity – >250 mAh/g (2.5-4.8V, 0.1C) intrinsic to lithium manganese  
175 rich cathode materials. The influence of addition of different solvents on the viscosity and surface  
176 tension was studied. The ink prepared from mixture of sol and propylene glycol (1:1, weight ratio)  
177 meet the requirements for inkjet printing. Thin film was printed with use of chosen ink.  
178

179 **Acknowledgments:** The team of authors is grateful to Zhejiang Changxing CHN-RUS New Energy and  
180 Material Technology Research Institute Co., Ltd, Republic of China for financial support in the research work  
181 under the contract between Zhejiang Changxing CHN-RUS New Energy and Material Technology Research  
182 Institute Co ., Ltd, Republic of China and St. Petersburg Polytechnic University of Peter the Great dated April  
183 21, 2017.

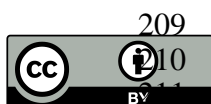
184 **Author Contributions:** M.M., Y.K. and A.V. conceived and designed the experiments; I.M., D.K., A.R.  
185 performed the experiments; I.M., A.R. and D.K. analyzed the data; A.P. contributed reagents, materials and  
186 analysis tools, D.K. and I.M. wrote the paper. M.M. and Y.K. reviewed the article.

187 **Conflicts of Interest:** The founding sponsors had no role in the design of the study; in the collection, analyses,  
188 or interpretation of data; in the writing of the manuscript, and in the decision to publish the results.  
189

190 **References**

- 191 1. Delannoy, P-E.; Riou, B.; Brousse, T.; Le Bideau, J.; Guyomard, D.; Lestriez, B. Ink-jet printed porous  
192 composite LiFePO<sub>4</sub> electrode from aqueous suspension for microbatteries. *Journal of Power Sources* **2015**,  
193 287, 261-268, DOI: [10.1016/j.jpowsour.2015.04.067](https://doi.org/10.1016/j.jpowsour.2015.04.067).
- 194 2. Johnson C.S.; Kim J-S.; Lefief C.; Li N.; Vaughey J.T.; Thackeray M.M., The significance of the Li<sub>2</sub>MnO<sub>3</sub>  
195 component in 'composite' xLi<sub>2</sub>MnO<sub>3</sub>•(1-x)LiMn<sub>0.5</sub>Ni<sub>0.5</sub>O<sub>2</sub> electrodes, *Electrochem. Commun.* **2004**, 6,  
196 1085-1091, DOI:10.1016/j.elecom.2004.08.002.
- 197 3. Thackeray M.M.; Kang S.-H.; Johnson C. S.; Vaughey J. T.; Benedekac R.; Hackneyb S. A.  
198 Li<sub>2</sub>MnO<sub>3</sub>-stabilized LiMO<sub>2</sub> (M = Mn, Ni, Co) electrodes for lithium-ion batteries. *J. Mater. Chem.* **2007**,17,  
199 3112-3125 DOI: 10.1039/b702425h.
- 200 4. Wang Qingsheng W.; Popovich A.; Zhdanovc V.; Novikov P.; Maximov M.; Koshtyal Yu.; Rummyantsev  
201 A.; Silin A. Synthesis of Li-ion Battery Cathode Materials Based on Lithiated Transition Metal Oxides by  
202 Spray Method *Russ J Appl Chem.* **2017**, 91, 53–57 DOI: 10.1134/S1070427217010081.
- 203 5. Roziera P.; Tarascon J-M. Review –Li-Rich Layered Oxide Cathodes for Next-Generation Li-Ion Batteries:  
204 Chances and Challenges *J. Electrochem. Soc.* **2015**, 162, A2490-A2499 DOI:10.1149/2.0111514jes.
- 205 6. Makhonina E.V.; Maslennikova L.S.; Volkov V.V.; Medvedeva A.E.; Rummyantsev A.M.; Koshtyal Yu. M.;  
206 Maximov M.Yu.; Pervov V.S.; Eremenko I.L.; Li-rich and Ni-rich Transition Metal Oxides: Coating and  
207 Core-Shell Structures *Appl. Surf. Sci., In Press*.

208



© 2018 by the authors. Submitted for possible open access publication under the terms and conditions of the Creative Commons Attribution (CC BY) license (<http://creativecommons.org/licenses/by/4.0/>).